Sensors and Materials, Vol. 12, No. 1 (2000) 015–024
MYU Tokyo

S & M 0393

Thick-Film Ultrasonic Transducer with Integrated Temperature Detector

Damiano Crescini, Daniele Marioli and Andrea Taroni

Department of Electronics for Automation, Faculty of Engineering,
University of Brescia, Via Branze 38 - 25123 Brescia, Italy

(Received January 22, 1999; accepted January 31, 2000)

Key words: ultrasonic sensors, thick-film technology, piezoelectric inks

The piezoelectric properties of thick-film inks based on lead zirconate titanate (PZT) have been used for developing a novel ultrasonic (US) transducer operating in air. The vibrating head consists of a 96% alumina disc actuated on the lower side by ferroelectric layers. In order to achieve compensation of the echo signal delay in the time-of-flight measurements (which closely follows the temperature dependence of the sound velocity) a nickel-based resistance temperature detector (RTD) is screen-printed and fired on the free side of the vibrating ceramic substrate. The design of the transducer is presented, together with the manufacturing procedures in thick-film technology. Moreover, frequency characterizations, radiation response and sound-pressure level (SPL) are reported for sensor operation in a silent box. As a proximity sensor, the US sensor developed has been tested in the temperature range from −10°C to +110°C. The error in the measured distance is maintained within ± 1.5% of the reading value. The sensor can be inexpensive enough to be competitive with other types of US sensors.

1. Introduction

In an ultrasonic (US) system, there must be a means of producing, receiving and displaying US signals. Three general types of transducers (magnetostrictive, electrostatic and piezoelectric) are used for the transduction of electric and mechanical energy.

Magnetostrictive transducers, typically made of nickel and nickel alloy,[1,2] are rarely used, except for high power systems (i.e., very-low-frequency nonimaging systems). Electrostatic transducers[3] (usually consisting of a Kapton, gold coating and aluminum plate) present no ringing effects and have a large usable frequency band. However, they require high DC bias and show a lower cost/performance ratio compared to piezoelectric devices.

Piezoelectric transducers are smaller and more efficient than electrostatic transducers. Certain naturally occurring crystals, such as quartz and tourmaline, are piezoelectric by virtue of their anisotropic atomic orientation. Beside these crystals, which can be designed as transducers for US, different ferroelectric ceramics, such as a mixture of lead, zirconate and titanate, are also used as US transducers because of their high Curie temperature. Baudry[4] and Prudenziati and Morten[5] demonstrated that piezoelectric layers can be prepared at a low cost using lead-zirconate-titanate (PZT)-based thick-film ink.

In the most popular application of the US sensors (e.g., in industrial-level measurements and/or distance detection),[6,7] the operating principle is very simple and is well known as a time-of-flight (TOF) technique. A short train of ultrasonic waves is generated by a piezoelectric device, travels through the medium, is reflected by the surface of the target, and then returns to the receiver and is detected. The time elapsed between the transmission and detection of the waves is a measure of the path traveled by the ultrasonic wave and consequently, of the distance of the reflecting surface from the transmitter/receiver system. In industrial systems, the same piezoelectric transducer works as both a transmitter and a receiver, the two functions being mechanically switched. Usually, the decrease of the echo amplitude at high temperatures does not affect the sensor performance except for a slight reduction of the maximum measurable distance of the target in distance or proximity measurements. In contrast, the temperature dependence of the TOF, which closely follows the temperature dependence of the sound velocity in air,[8] affects the accuracy of the US sensor unless it is electronically compensated. On this basis, this paper briefly presents a novel ultrasonic thick-film transducer operating in air actuated by PZT layers with an integrated nickel-based RTD sensor for compensation of temperature effects.

2. Design and Manufacture of Thick-Film US Transducer

To generate any kind of mechanical wave, including US waves, the movement of a surface is required. This movement causes compression and expansion of a medium, which can be gas (air), liquid or solid.

The thick-film transducer (TFT) design features a ceramic disc bender that is maintained in resonance at a nominal frequency of 25, 33 or 40 kHz and radiates or receives ultrasonic energy. The US transmitter/receiver sensor developed in our laboratory is manufactured by screen-printing and firing special thick-film ink onto a 96% alumina (Al_2O_3) disc.[9] A sketch of the transducer is shown in Fig. 1. The active elements have a structure comprising a plane capacitor consisting of ferroelectric layers as the dielectric and two conductive plates based on Pd/Ag material (*Heareus C1214*), as armatures. In order to achieve adequate piezoelectric characteristics, after the firing processes (at a peak temperature of about 950°C) the layers were subjected to a poling process by applying a DC electric field of 1.7 MV/m at 200°C for 20 min. The field was removed after the layers had cooled to room temperature. These procedures induced the piezoelectric activity of the layers which exhibit a g_{33} voltage coefficient of about 70×10^{-3} Vm/N, a dielectric constant of approximately 300 and an electromechanical coupling factor $k_{33} = 0.49$ (g_{33} and k_{33} are measured as explained in refs. (5) and (10).

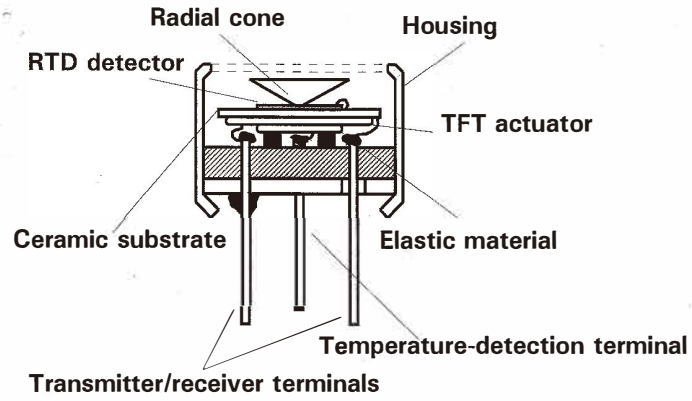

Fig. 1. Schematic of the thick-film US transducer.

The resistance temperature detector (RTD), which is required to reveal the variations in environmental conditions, is based on an air-fired nickel conductor (*ESL 2557*). The fired nickel film has a high, positive temperature coefficient of resistance and is a suitable candidate for commercial temperature-sensing applications. This conductor is terminated onto silver (*ESL 9901*) to give a solderable connection.

Figure 2 shows a photograph of the TFT prototypes of the US transducer together with the radial cone and the metal housing. The ferroelectric active layer (top right) and the RTD detector with the spiral shape (top left) are clearly distinguishable. Moreover, on the photograph other samples are reported with different diameters. The aim was to cover resonance frequencies up to 40 kHz.

Adopting ceramic circular substrates with three different diameters (thickness $t_{Al_2O_3}$ = 220 mm, density $\rho_{Al_2O_3}$ = 3.8 kg/dm^3 and Young's modulus $Y_{Al_2O_3}$ = 330 MPa) and taking into account the geometrical constitutive characteristics of the PZT layers (total thickness t_{PZT} near 170 μm, density ρ_{PZT} of about 7.9 kg/dm^3, Poisson's ratio υ_{PZT} = 0.31 and Young's modulus Y_{PZT} = 15–20 MPa) typical operating frequencies of 25, 33 and 40 kHz are obtained. The US frequency used corresponds to the first vibration mode[11,12,13] of a free-edge circular diaphragm. The deformed shape shows a radial symmetry with a single circular nodal line positioned at 0.3 d with respect to the center. The nodal line is used to glue the ceramic disc elastically to the support base.

3. Experimental Results

In Table 1, the resonant frequencies predicted theoretically, determined by the finite-element method (FEM) and measured experimentally are given. Based on the data obtained, we can observe that the values of resonant frequencies calculated using the

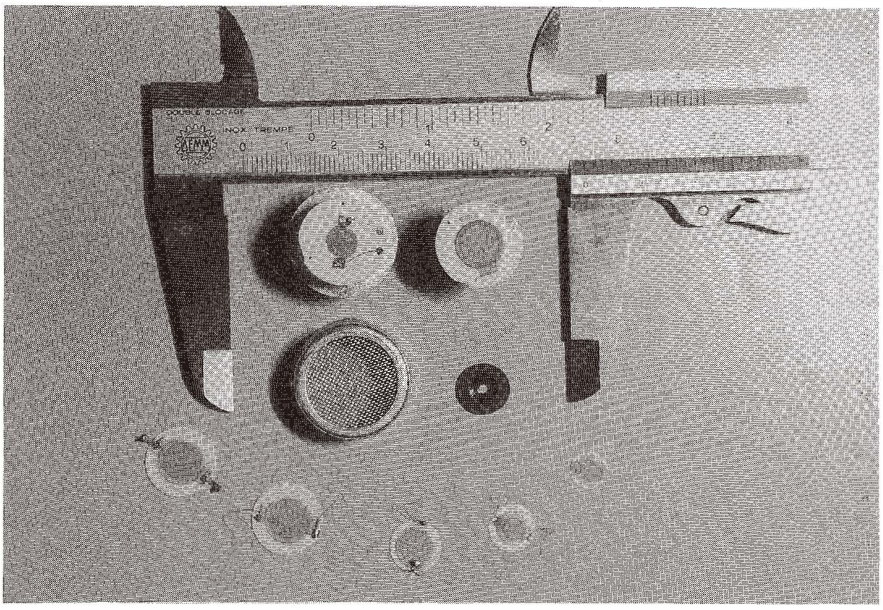

Fig. 2. Photograph of the US prototypes developed.

Table 1
Resonance frequency of the 25, 33, 40 and 47 kHz TFT prototypes.

	Resonance frequency		
Prototype	Classic formulae	FEM analysis	Measured data
TFT 25	26.704 kHz	25.612 kHz	25.975 kHz
TFT 30	31.843 kHz	30.043 kHz	30.550 kHz
TFT 40	41.316 kHz	39.737 kHz	40.325 kHz
TFT 47	48.105 kHz	47.905 kHz	47.575 kHz

classic approach (defining an equivalent rigidity of the bimorphs plate and considering the clamping conditions[11,12,13]) are higher than those of the measured values (+8%). One possible reason is that the analytical method assumes the uniform geometrical distribution of the PZT layers without considering the clamping effects. Using FEM analysis, better agreement with the observed values can be achieved (numerical modeling could better reproduce the mass distribution and clamping conditions).

Figure 3 shows the impedance-phase spectra for the case of the 40-kHz TFT prototype. The impedance curve presents a minimum at the resonance frequency of about 700 Ω, while at the antiresonance frequency, an impedance of about 8 kΩ is found.

An example of the experimental test setup for evaluating the thick-film prototype used

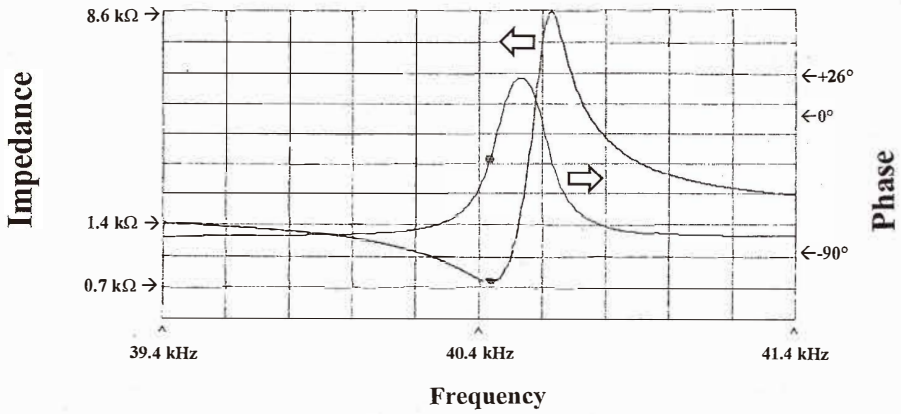

Fig. 3. Impedance/phase spectra of the 40 kHz TFT prototype.

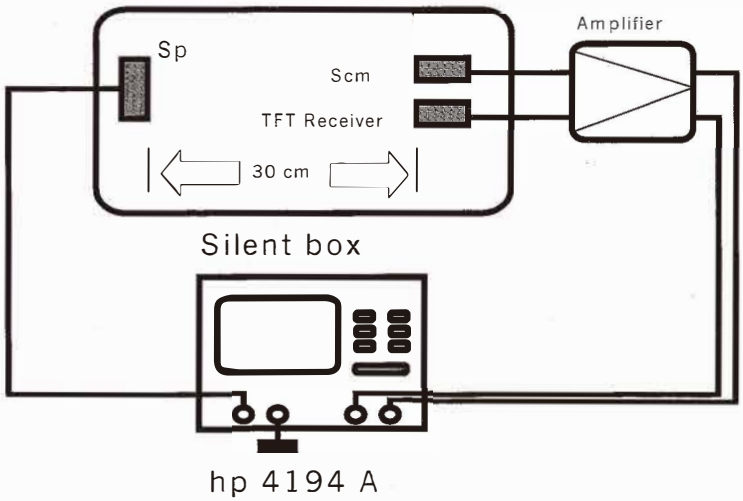

Sp : Tweeter
Scm : Standard Condenser Microphone (B&K 4135)
TFT : Thick-Film

Fig. 4. Example of the experimental setup for measuring the TFT receiver sensitivity.

in the receiver mode is illustrated schematically in Fig. 4.

A general idea of the thick-film sensor performance for the 25 kHz prototype can be deduced from Table 2, where all values were obtained under the following standard conditions: the transducer is supplied with 10 Vrms, the distance between the transmitter and the microphone is maintained at 0.30 m and a free-field 1/4-inch microphone, B&K 4153, is used for reference (sensitivity of about 4 mV/Pa with a frequency range from 4 Hz to 100 kHz).

In Fig. 5, the radiation characteristic for the 40 kHz TFT prototype obtained upon mounting a plastic radial cone on the upper side of the circular substrate, is presented. A 10

Table 2
Thick-film US sensor performance.

Parameter	Measured performance
Nominal frequency	25 kHz
Sensitivity	–75 dB/V/microbar min.
Bandwidth	4 kHz min. at –80 dB
Capacitance	1400 pF
Insulation resistance	more than 100 MΩ
Sound level	116 dB max.
Temperature characteristic	15 dB at –15°C to 60°C

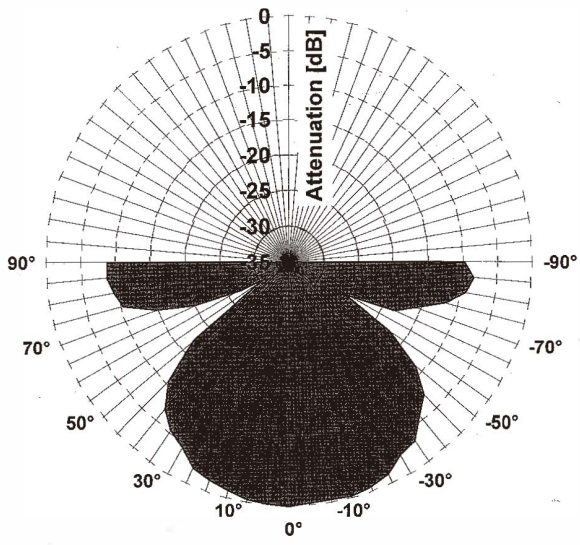

Fig. 5. Radiation characteristic of the 40 kHz TFT prototype.

dB attenuation is found at 45° degrees with respect to the 0 dB axis.

Figure 6 shows the sound-pressure level (SPL) measured with a silent box in which the developed thick-film prototype is used as a transmitter. A 116 dB level is found in the case of 24,700 Hz.

Figure 7 shows the frequency response of the 40 kHz TFT prototype when it is used as a receiver. A sensitivity of –75 dB/V/μbar min can be observed with a corresponding bandwidth of about 4 kHz min at –80 dB.

The sensitivity variation has been evaluated during a temperature cycle from –10°C to 100°C. To perform the measurements, the silent box was placed in a chamber with controlled atmosphere. An attenuation within 20 dB is found under all conditions. The characterizations of the nickel-based RTD sensor show a sensitivity of about 1.1 Ω/°C with a resolution near 0.2°C (adopting the resistance Ro ≅ 150 Ω at 25°C). A three-wires

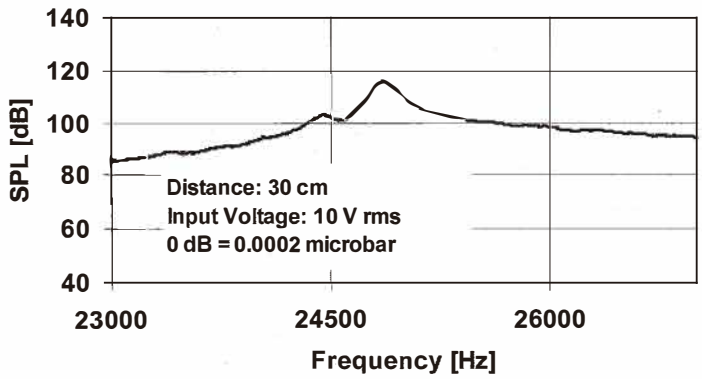

Fig. 6. Sound pressure level (SPL) of the 40 kHz TFT prototype.

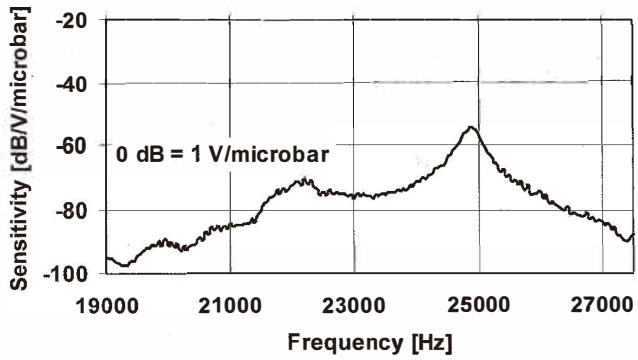

Fig. 7. Sensitivity behavior of the 40 kHz TFT prototype.

measurement has been adopted.

Figure 8 shows an example of the SPL in the case of a 40 kHz TFT prototype vs the input voltage applied to the sensor. A maximum value of about 120 dB is observed with a 40 V input.

Finally, Fig. 9 shows an example of reading errors in distance measurement as a function of ambient temperature when the dependence of the sound velocity is compensated using the built-in RTD sensor; closed circles refer to the uncompensated measure-

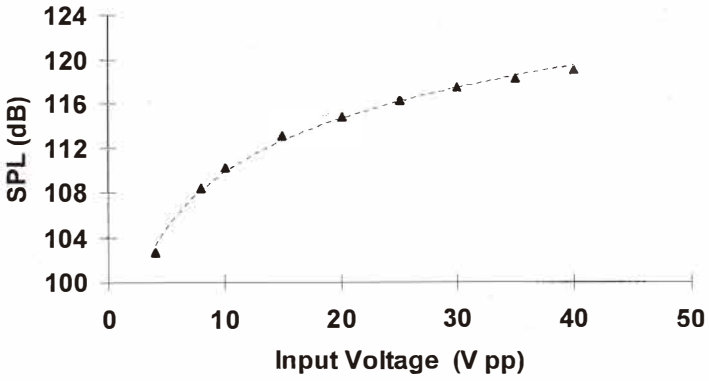

Fig. 8. Sound pressure level (SPL) vs input voltage for the 25 kHz TFT prototype.

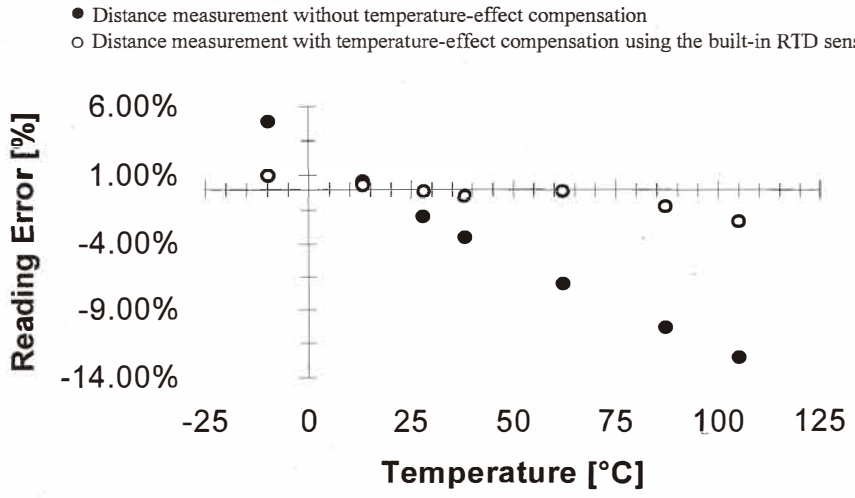

Fig. 9. Reading errors of the sensor as a function of ambient temperature.

ment whereas the open circles refer to the electronically compensated measurement. As shown in the figure, the error is always lower than ±1.5% of the reading value in the temperature range from –10°C to 110°C. The target was preset by D = 60 cm, and the transducer adopted was the 40 kHz TFT prototype.

The electronic device for the temperature-effect compensation was based on a 68HC11 Motorola single-chip microcontroller and a NE555 counter. For this purpose, a resistive network (Fig. 10) was used, including a built-in thick-film sensor which supplies the temperature-dependent voltage V_T.

The voltage V_T drives the NE555 counter connected to a voltage-controlled oscillator (VCO) so that the frequency will change with temperature in order to balance the temperature dependence of the sound velocity.

Analogously, the operation of the sensor can be compensated for changes other than physical quantity such as humidity using an appropriate built-in thick-film humidity sensor.

4. Conclusions

We briefly described a potential multifunctional US piezoelectric device for remote control, as well as distance and proximity measurements, developed using thick-film technology.

Piezoelectric ink, based on PZT, has been used to actuate and/or receive US waves. To overcome the temperature dependence of the echo signal delay in the TOF measurements (which closely follows the temperature dependence of the sound velocity) a nickel-based

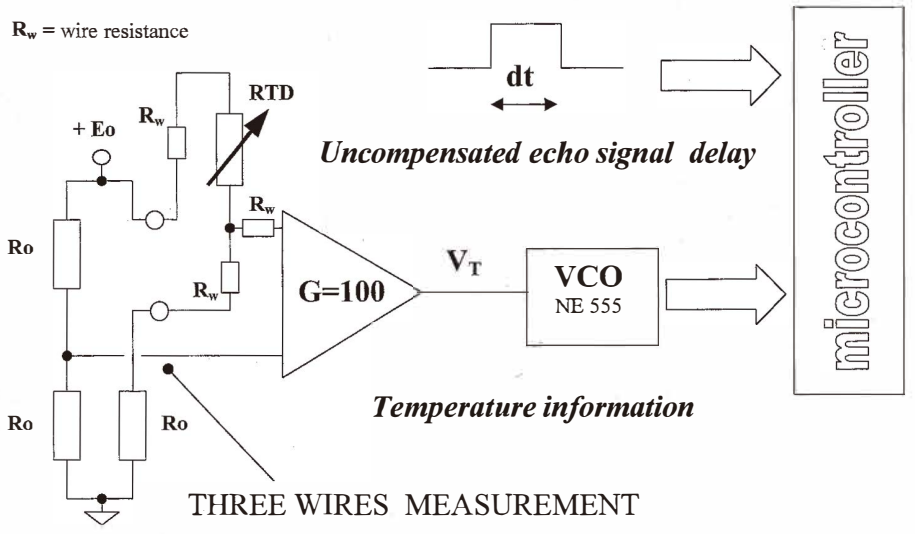

Fig. 10. Schematic of temperature-effect compensation circuit.

RTD sensor was screen-printed and fired on the free side of the vibrating ceramic substrate. As a proximity sensor, the US sensor developed was tested in the temperature range from –10°C to +110°C. The error in the measured distance is maintained within ±1.5% of the reading value.

Resonance frequencies of 25, 33 and 40 kHz were obtained through a simple rearrangement of the substrate (Al_2O_3) geometry. A minimum sensitivity of –75 dB/V/μbar min and a SPL near 116 dB max were easily achieved and good directivity can be observed.

Finally, the sensor is inexpensive enough to be, in the near future, highly competitive with other types of commercial US transducers; moreover, if we utilize the thick-film US head equipped with a low-cost capacitive humidity sensor (e.g., one obtained by screen printing and firing an interdigitate capacitive sensor), complete compensation with regard to environmental conditions can be achieved.

References

1 T. F. Hueter and R. H. Bolt: Sonics (Wiley, New York, 1955) Chap. 5.
2 L. Cremer and M. Heckl: Körperschall (Springer, Berlin, 1967) p. 65.
3 C. Biber, S. Ellin, E. Shenk and J. Stempeck: The POLAROID Ultrasonic Ranging System, 67th AES Convention (New York, 1980) p. 233.
4 H. Baudry: 6th Europ. Microel. Conf. (Bounemount, 1987) p. 456.
5 M. Prudenziati and B. Morten: 7th Europ. Microel. Conf. (Hamburg 1989) p. 86.
6 D. Marioli, E. Sardini and A. Taroni: IEEE Trans. on Instrum. Meas. IM-**37** (1988) 53.
7 V. Magori and P. Kleinschmidt: Siemens Forsch. u. Entwickl.-Ber. **10** (1981) p.110.
8 B. Carlin: Ultrasonics (McGraw-Hill, New York, 1960)
9 M. Prudenziati and B. Morten: Sensors and Actuators A **21–23** (1990) 47.
10 M. Prudenziati and B. Morten: 8th Europ. Microel. Conf. (Rotterdam, 1991) p. 122.
11 W. C. Young: Roark's Formulae for Stress and Strain (McGraw-Hill, New York, 1989) p. 89, 102, 104.
12 L. E. Kinsler, A. R. Frey, A. B. Coppens and J. V. Sanders: Fundamentals of Acoustics (John Wiley & Sons, New York, 1982) p. 233.
13 R. D. Blevins: Formulas for Natural Frequency and Mode Shape (Krieger, Malaba, 1987) p. 418.